

PROCEEDINGS OF SPIE

[SPIDigitalLibrary.org/conference-proceedings-of-spie](https://spiedigitallibrary.org/conference-proceedings-of-spie)

Flexible waveguides with amorphous photonic materials

Murat Can Sarihan, Yildirim Batuhan Yilmaz, Mertcan Erdil, Mehmet Sirin Aras, Cenk Yanik, et al.

Murat Can Sarihan, Yildirim Batuhan Yilmaz, Mertcan Erdil, Mehmet Sirin Aras, Cenk Yanik, Chee Wei Wong, Serdar Kocaman, "Flexible waveguides with amorphous photonic materials," Proc. SPIE 10914, Optical Components and Materials XVI, 1091410 (27 February 2019); doi: 10.1117/12.2510685

SPIE.

Event: SPIE OPTO, 2019, San Francisco, California, United States

Flexible waveguides with amorphous photonic materials

Murat Can Sarihan^{*a}, Yildirim Batuhan Yilmaz^{*b}, Mertcan Erdil^b, Mehmet Sirin Aras^a, Cenk Yanik^c, Chee Wei Wong^a, and Serdar Kocaman^b

^aMesoscopic Optics and Quantum Electronics Laboratory, Department of Electrical and Computer Engineering, University of California, Los Angeles, USA

^bQuantum Devices and Nanophotonics Research Laboratory, Department of Electrical and Electronics Engineering, Middle East Technical University, Ankara, Turkey

^cSabancı University Nanotechnology Research and Application Center, Sabancı University, Istanbul, Turkey

ABSTRACT

Amorphous photonic materials offer an alternative to photonic crystals as a building block for photonic integrated circuits due to their shared short-range order. By using the inherent disorder of amorphous photonic materials, it is possible to design flexible-shaped waveguides that are free from restrictions of photonic crystals at various symmetry axes. Effects of disorder on photonic crystal waveguide boundaries have been examined before, and it is shown that flexible waveguides with high transmission are possible by forming a wall of equidistant scatterers around the defect created inside amorphous material configuration. Based on this principle, waveguides with various flexible shapes are designed and fabricated for planar circuit applications. A silicon-on-insulator (SOI) slab with random configuration of air hole scatterers is used. The amorphous configuration is generated through realistic Monte Carlo simulations mimicking crystalline-to-amorphous transition of semiconductor crystals via an assigned Yukawa potential to individual particles. The design parameters such as average hole distance, slab thickness and hole radius are adjusted so that the waveguide is utilizable around 1550 nm telecommunications wavelength. Such waveguides on slab structures are characterized here and the level of randomness and band gap properties of amorphous configurations are analyzed in detail. These efforts have the potential to lead easier design of a wide range of components including but not limited to on-chip Mach-Zehnder interferometers, splitters, and Y-branches.

Keywords: Photonic bandgap materials, waveguides, photonic crystals, amorphous photonic materials, disorder

1. INTRODUCTION

Photonic crystals (PhC) allow confinement of certain frequencies of light by forming a bandgap, which makes them useful for many applications, including filters and waveguides.^{1,2} Photonic bandgaps (PBG) of photonic crystals stem from periodic arrangement of the dielectric structure. With the invention of the first 3-D photonic crystal three decades ago,³ the photonic crystals took a lot of attention from the various research groups since then³⁻⁸ and utilization of photonic crystal devices for photonic integrated circuit applications intensified. The disadvantage of photonic crystal devices is that the light confinement depends on the preservation of symmetry and periodicity. As a result, the defects formed in crystal lattice for light propagation, should follow the main symmetry axes. Thus, it is not possible to use PhC's for designing arbitrarily shaped waveguides.

Similar to electronic bandgaps formed in amorphous semiconductors, amorphous photonic lattices also exhibit PBG property. Although amorphous distributions lack a long-range order, their short-range order which is shared by periodic counterparts results a bandgap.⁸ Following this idea, bandgaps in amorphous structures were theoretically explored more than four decades ago, and later experimentally proved on amorphous semiconductors.^{9,10} Recently, the implementations of 2-D and 3-D amorphous photonic materials with photonic bandgaps in the microwave and optical wavelengths have been studied^{5,8,11} and preliminary studies in the infrared regime have been also conducted.¹² Amorphous photonic lattices being symmetry independent makes them convenient for design and fabrication of photonic integrated circuits. The initial studies show theoretically that the amorphous PBG can be utilized by defects to guide the light. In previous studies, the effects of disorder on photonic

crystal waveguides and possible design schemes for amorphous waveguide configurations have been shown. Here, we would like to present a roadmap to design amorphous waveguides with flexible shapes. The initial studies provide transmission rates higher than 70% for bends with any arbitrary angles. Such structures are good candidates to use in main photonic integrated circuit applications such as switches, modulators, interferometry and coupling, while also enables the study of localization phenomenon in the light propagation.

2. DESIGN OF FLEXIBLE WAVEGUIDE STRUCTURES

In order to design photonic band gaps with amorphous structures, photonic crystals are used as a reference due to the fact that the first band gap of the PhC originates from short-range order.⁸ In order to achieve that, the design parameters, lattice constant (a) (i.e. average distance between holes in amorphous configuration), thickness (h) and hole radius (r), are kept constant for both photonic crystal and amorphous structure. For this purpose, band diagrams of various photonic crystal configurations have been numerically calculated with M.I.T. Photonic-Bands (MPB) software¹³ for the transverse electric (TE) modes. Consequently, the transmission spectra and field distributions are obtained by finite-difference time-domain method (FDTD) using M.I.T. Electromagnetic Equation Propagation (MEEP) software¹⁴ in order to verify the band gaps. The design parameters which provides a band gap around C-L bands are used to construct the amorphous configuration of refractive index over the slab.

The amorphous refractive index distributions are prepared by Metropolis Monte Carlo simulations via LAMMPS package.^{11,15,16} In these simulations, air holes are represented as particles in a liquid-like medium and crystalline-to-amorphous transition is achieved. The initial photonic crystal configuration is disturbed and evaluated until statistical equilibrium according to Metropolis criterion, which is $acc(1 \rightarrow 2) = \min(1, e^{-[U(2)-U(1)]/k_B T})$. The criterion assigns an acceptance probability to each displacement attempt according to the change in the potential energy of the lattice that the displacement causes.¹⁵ Here, U is the potential energy of initial and final configurations, while the k_B is Boltzmann constant and T is temperature.

The potential energy of the lattice is calculated by Yukawa potential energy function, $v(r) = \frac{v_0}{r} e^{-r/l}$, $r < r_0$, which is used for colloidal interactions.^{11,17} The short-range order is adjusted by the normalized temperature parameter $T^* = k_B T / v_0$ where l represents the screening length in the configuration and v_0 is a multiplier constant for the potential. The generated configurations are scaled by using the lattice constant of the reference photonic crystal.

Waveguides are essentially line defects that are perturbing the order of the lattice. They can also be represented as the point defects that are coupled to each other.¹⁸ Fig. 1 provides a sample waveguide for PhC and amorphous structures. As a result, we observe defect modes in the PBG region of the band diagram, which enables transmission. For the photonic crystal waveguides, this mode is due to broken discrete translational symmetry along the propagation direction, while the symmetry is conserved at transverse direction. The number of

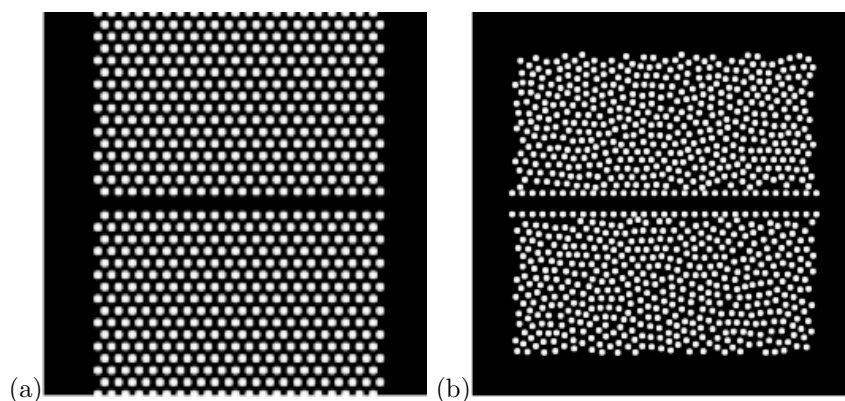


Figure 1: Refractive index distribution of (a) PhC waveguide and (b) amorphous waveguide. White regions represent air holes and black regions represent silicon (Si) slab. The regions at the edges without holes are PML layers.

modes that can be propagated through the waveguide is determined by the number of lines that the defect is formed.⁴ This property provides us the means to design a high-performance waveguide but only along the main symmetry axes of the photonic crystal lattice.

The effects of lattice disturbance on the photonic crystal waveguides have been examined before and shown that the first band gap is very robust against disorder when it is utilized for waveguides.¹⁹ On the other hand, amorphous structures have no such symmetry. Thus, the light can be transmitted through a waveguide in amorphous material, along any arbitrary direction by using that first band gap shared by the amorphous lattice due to the short range order.⁸ The mechanism that enables such transmission lies in the Anderson localization phenomenon.^{11,20–22} The theory of localization states that for any amount of disorder, the mode of light becomes localized for a finite length.^{23,24} Thus a defect formed inside an amorphous materials would create a localized mode. The coupling of consecutive localized modes that each of them are created by a point defect, can support an extended mode that enables propagation.

Waveguides, in amorphous lattice, are formed by removing holes from a certain region. The possible issue is that the waveguide width may slightly vary due to random positions of removed holes. In order to avoid local reflections due to impedance change, we have placed a wall of equidistant holes around the waveguide region. This method is implemented and deemed as effective by a previous study on arbitrary-shaped waveguides based on uniformly distributed scatterers having neither short- nor long-range order.²⁵

3. RESULTS AND DISCUSSIONS

As the initial step, the waveguides in an amorphous material are numerically analyzed in terms of transmission versus waveguide width and bending angle. Furthermore, the straight waveguides in amorphous materials are compared with their photonic crystal counterparts, which can be seen in Fig. 2.

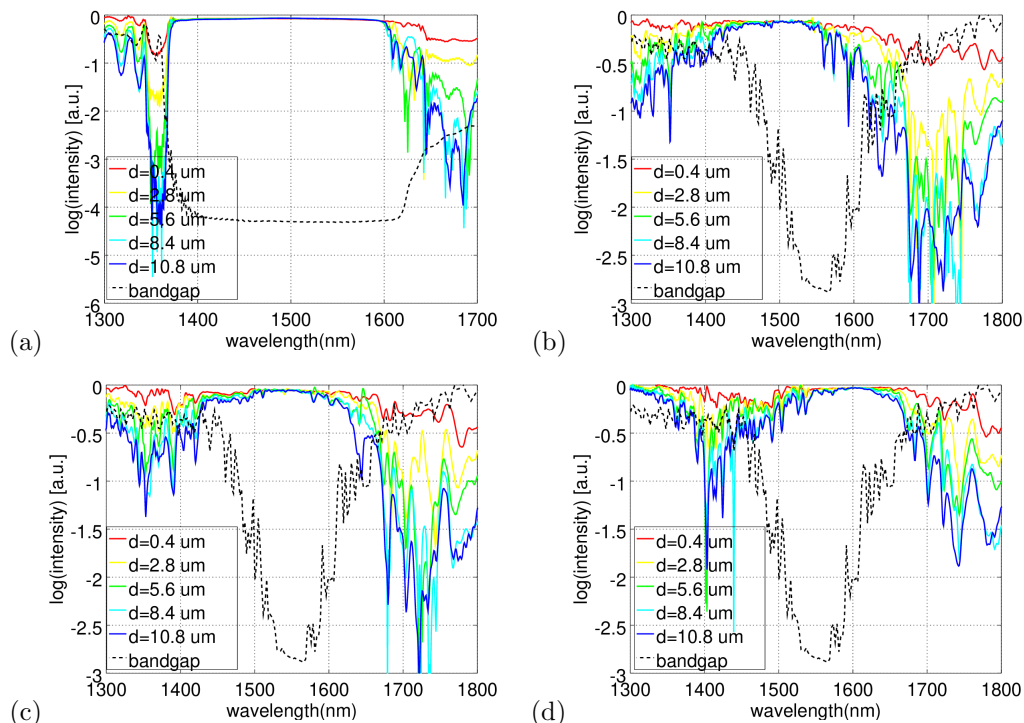


Figure 2: Transmission spectra of (a) straight PhC waveguide with width 831 nm, (b-d) amorphous waveguide with widths 831, 901 and 970 nm respectively, at various distances from the source.

It has been known that adjusting width of the line defect in PhC waveguides plays a huge role in altering the frequency range of the defect mode,²⁶ which is shown here that also the case for amorphous waveguides. In a

photonic crystal, removing holes like in Fig. 1 results a defect waveguide with width $\sqrt{3}$ times the lattice constant a . However available modes in this defect may not necessarily support the desired frequency range. To adjust defect frequency, width of the waveguide can be adjusted. In this work, transmission spectra of $1.2\sqrt{3}a$ (831 nm), $1.3\sqrt{3}a$ (901 nm) and $1.4\sqrt{3}a$ (970 nm) thick straight waveguides were analyzed.

Transmission spectrum of the amorphous waveguides are shown in Fig. 2. The waveguides can confine the light with low loss around the center of the passband. Bandwidth of the waveguide maximizes as center frequency of the defect mode overlaps with center of the bandgap. Transmission spectra of the 901 nm wide waveguide in Fig. 2c has full width at half maximum (FWHM) value 203 nm at $d = 10.8 \mu\text{m}$ whereas transmission spectra of the 831 and 970 nm wide waveguides shown in Fig. 2b and Fig. 2d have a FWHM value around 150 nm. Transmission spectrum of the PhC waveguide is also shown with amorphous waveguides for comparison. Flat bandgap of the PhC results to a flat passband for the waveguide. Since the bandgap transition of the PhC lattice at the edge of air band is sharper, this also results a sharper transition at the passband of the waveguide.

Field distributions of the waveguides with 3 different widths are shown in Fig. 3. It can be seen that transmission is best at 901 nm wide waveguide, because the frequency of the TE wave matches with the center frequency of that waveguide, which is easy to comprehend from Fig. 2. At other waveguides, the light couples to cavities around the waveguide significantly more. Cavities either exist in the amorphous configuration or they occur because of the gap formed by removed holes between amorphous lattice and the holes at the edge of the waveguide. For a good transmission rate, density of cavities must be as low as possible and frequency of the guided mode must match with the waveguide.

To bend the waveguide, a circular section is placed between two straight sections. This provides a smooth transition with less reflections. Number of holes at the inner and outer edges of the section is adjusted so that distance between the holes is as close to the lattice constant as possible. Field distribution and transmission spectrum of a waveguide bend is given in Fig. 4. In the field distribution, it is observed that coupling to cavities around the waveguide considerably increase at the bend. The fluctuations in the transmission spectrum is also a probable result of cavities around the bend. The impedances of circular and straight sections must be as close as possible.

Comparison of transmission rates of different bends are demonstrated in Fig. 5. Using a suitable radius of curvature, one can obtain a good transmission rate for any angle. At some angles, even 100% transmission is

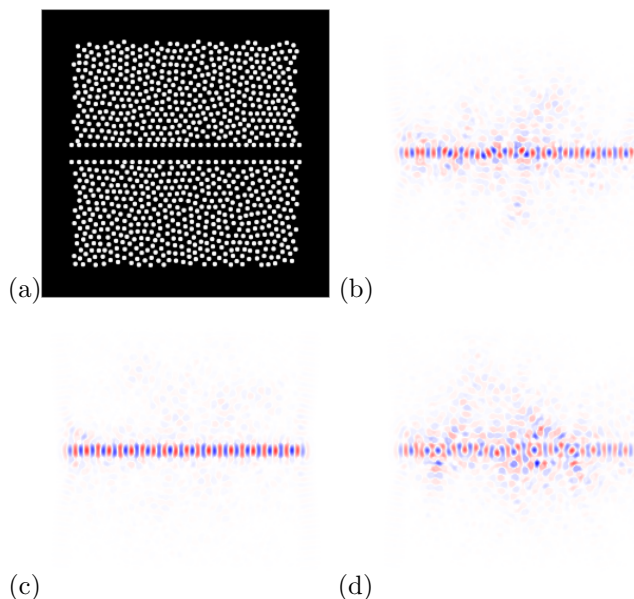


Figure 3: An example of a straight waveguide and field distributions in waveguides with different widths. (a) Refractive index distribution of amorphous waveguide (top view). (b-d) Field distribution of a 1550 nm TE wave in waveguides with widths 831 nm, 901 nm and 970 nm respectively.

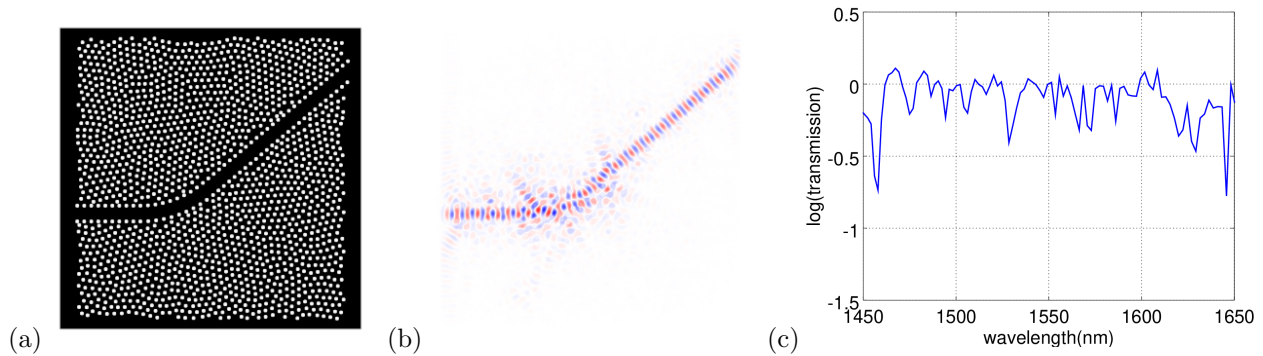


Figure 4: (a) Refractive index distribution amorphous waveguide bend with 40 degrees and radius of curvature set to $15a$. (b) Field distribution of a 1550 nm TE wave in the amorphous waveguide bend. (c) Transmission spectrum of the amorphous waveguide bend.

possible. Among the reasons of additional losses, deviation from the inherent short-range order of the amorphous configuration due to the wall around waveguide, location and density of the cavities formed around the waveguide may have an effect on the transmission through the bends, which can lead to power coupling.

The opportunity of being able to design waveguide bends at any desired angles is the superior advantage of amorphous waveguides. This flexibility in waveguide structure can simplify the design of on-chip photonic integrated circuits.

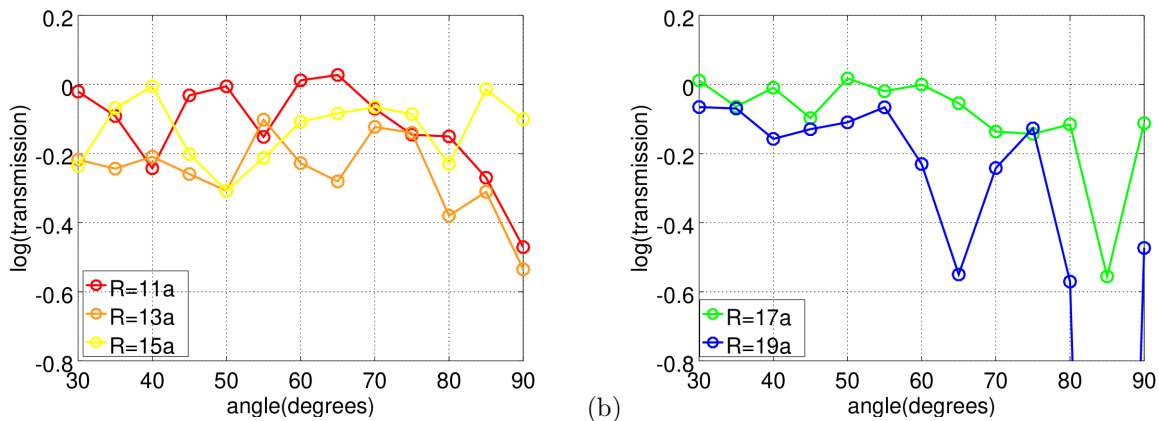


Figure 5: Transmission rates of bends with different radii of curvature(R) and different angles for 1550 nm TE wave

4. CONCLUSIONS

Here, we offer a pathway to design and implement practical flexible waveguides by utilizing amorphous materials. Amorphous waveguides bring many opportunities for photonic integrated circuit applications, especially for switches, modulators and interferometers. It has been demonstrated numerically that amorphous photonic materials can be used to confine light by forming waveguides with line defects. Such waveguides can be optimized to have low loss over C and L bands with small bending losses. The bends formed by waveguides can have arbitrary angles with high transmission rates.

ACKNOWLEDGMENTS

This work was supported by the Scientific and Technological Research Council of Turkey (TUBITAK), Grant No: 117E178.

REFERENCES

- [1] Costa, R., Melloni, A., and Martinelli, M., “Bandpass resonant filters in photonic-crystal waveguides,” *IEEE Photonics Technology Letters* **15**(3), 401–403 (2003).
- [2] Skivesen, N., Têtu, A., Kristensen, M., Kjems, J., Frandsen, L. H., and Borel, P. I., “Photonic-crystal waveguide biosensor,” *Optics Express* **15**(6), 3169–3176 (2007).
- [3] Yablonovitch, E., “Inhibited spontaneous emission in solid-state physics and electronics,” *Physical Review Letters* **58**(20), 2059–2062 (1987).
- [4] Joannopoulos, J. J. D., Johnson, S., Winn, J. N. J., and Meade, R. R. D., [*Photonic Crystals: Molding the Flow of Light*], Princeton University Press (2008).
- [5] Edagawa, K., Kanoko, S., and Notomi, M., “Photonic amorphous diamond structure with a 3D photonic band gap,” *Physical Review Letters* **100**(1), 1–4 (2008).
- [6] Kocaman, S., Aras, M. S., Hsieh, P., McMillan, J. F., Biris, C. G., Panoiu, N. C., Yu, M. B., Kwong, D. L., Stein, A., and Wong, C. W., “Zero phase delay in negative-refractive-index photonic crystal superlattices,” *Nature Photonics* **5**(8), 499–505 (2011).
- [7] Govdeli, A., Sarihan, M. C., Karaca, U., and Kocaman, S., “Integrated optical modulator based on transition between photonic bands,” *Scientific Reports* **8**, 1619 (dec 2018).
- [8] Jin, C., Meng, X., Cheng, B., Li, Z., and Zhang, D., “Photonic gap in amorphous photonic materials,” *Physical Review B* **63**, 195107 (apr 2001).
- [9] Weaire, D. and Thorpe, M., “Electronic properties of an amorphous solid. i. a simple tight-binding theory,” *Physical Review B* **4**(8), 2508 (1971).
- [10] Cody, G., Tiedje, T., Abeles, B., Brooks, B., and Goldstein, Y., “Disorder and the optical-absorption edge of hydrogenated amorphous silicon,” *Physical Review Letters* **47**(20), 1480 (1981).
- [11] Rechtsman, M., Szameit, A., Dreisow, F., Heinrich, M., Keil, R., Nolte, S., and Segev, M., “Amorphous photonic lattices: band gaps, effective mass, and suppressed transport,” *Physical review letters* **106**(19), 193904 (2011).
- [12] Kocaman, S., McMillan, J. F., Wang, D., Rechtsman, M. C., and Wong, C. W., “Observation of band gaps in amorphous photonic structures with different temperatures in the near infrared,” *Conference on Lasers and Electro-Optics Europe - Technical Digest*, 2–3 (2014).
- [13] Johnson, S. and Joannopoulos, J., “Block-iterative frequency-domain methods for Maxwell’s equations in a planewave basis,” *Optics Express* **8**, 173 (jan 2001).
- [14] Oskooi, A. F., Roundy, D., Ibanescu, M., Bermel, P., Joannopoulos, J., and Johnson, S. G., “Meep: A flexible free-software package for electromagnetic simulations by the FDTD method,” *Computer Physics Communications* **181**, 687–702 (mar 2010).
- [15] Frenkel, D. and Smit, B., [*Understanding Molecular Simulation: From Algorithms to Applications*], vol. 1, Academic Press (2001).
- [16] “LAMMPS Molecular Dynamics Simulator.” Accessed on Jan 10, 2019.
- [17] Hynninen, A.-P. and Dijkstra, M., “Phase diagrams of hard-core repulsive Yukawa particles,” *Physical Review E* **68**(2), 021407 (2003).
- [18] Chien, F.-S., Tu, J., Hsieh, W.-F., and Cheng, S.-C., “Tight-binding theory for coupled photonic crystal waveguides,” *Physical Review B* **75**(12), 125113 (2007).
- [19] Kwan, K. C., Zhang, X., Zhang, Z. Q., and Chan, C. T., “Effects due to disorder on photonic crystal-based waveguides,” *Applied Physics Letters* **82**(25), 4414–4416 (2003).
- [20] Schwartz, T., Bartal, G., Fishman, S., and Segev, M., “Transport and Anderson localization in disordered two-dimensional photonic lattices,” *Nature* **446**(7131), 52–55 (2007).
- [21] Segev, M., Silberberg, Y., and Christodoulides, D. N., “Anderson localization of light,” *Nature Photonics* **7**(3), 197–204 (2013).
- [22] Hsieh, P., Chung, C., McMillan, J. F., Tsai, M., Lu, M., Panoiu, N. C., and Wong, C. W., “Photon transport enhanced by transverse Anderson localization in disordered superlattices,” *Nature Physics* **11**(3), 268–274 (2015).
- [23] Anderson, P. W., “Absence of diffusion in certain random lattices,” *Physical Review* **109**(5), 1492–1505 (1958).

- [24] Sarihan, M. C., *Photonic integrated circuit components with amorphous structures*, Master's thesis, Middle East Technical University, Ankara, Turkey (2018).
- [25] Miyazaki, H., Hase, M., Miyazaki, H. T., Kurokawa, Y., and Shinya, N., "Photonic material for designing arbitrarily shaped waveguides in two dimensions," *Physical Review B* **67**, 235109 (jun 2003).
- [26] Notomi, M., Yamada, K., Shinya, A., Takahashi, J., and Takahashi, C., "Photonic crystal waveguide," (Nov. 4 2003). US Patent 6,643,439.